EXAFS characterization of bimetallic Pt–Pd/SiO_2–Al_2O_3 catalysts for hydrogenation of aromatics in diesel fuel

Takashi Fujikawa *, Koji Tsuji, Hirofumi Mizuguchi, Hideki Godo, Kazuo Idei and Kazushi Usui

Cosmo Research Institute, 1134-2 Gongendo, Satte, Saitama 340-0193, Japan
E-mail: takashi_fujikawa@cosmo-oil.co.jp

Received 19 July 1999; accepted 22 September 1999

Bimetallic Pt–Pd/SiO_2–Al_2O_3 catalysts exhibited much higher activities in aromatic hydrogenation of distillates than monometallic Pt/SiO_2–Al_2O_3 and Pd/SiO_2–Al_2O_3 catalysts. The studies of extended X-ray absorption fine structure (EXAFS) indicated that there was an interaction between Pt and Pd in the Pt–Pd/SiO_2–Al_2O_3 catalyst. Furthermore, from the EXAFS, it was assumed that the active metal particle on the Pt–Pd/SiO_2–Al_2O_3 catalysts is composed of the "Pd dispersed on Pt particle" structure. Regarding both the activities of aromatic hydrogenation and the EXAFS results, it was concluded that the Pd species dispersed on Pt particles were responsible for the high activity of the bimetallic Pt–Pd/SiO_2–Al_2O_3 catalysts.

Keywords: Pt–Pd bimetallic catalysts, aromatic hydrogenation, diesel fuel, EXAFS, active site, Pd species dispersed on Pt particle

1. Introduction

A high aromatic content in diesel fuel lowers the fuel quality and it has been recognized to bring about the formation of suspended particulate matter in exhaust gases from diesel engines [1,2]. Therefore, much attention has been paid to the development of a new catalytic technology for aromatic hydrogenation in diesel fuel. Recently, extensive studies have been performed to develop sulfur-tolerant noble-metal catalysts for the two-stage hydrogenation process by a great number of researchers [3–28].

In particular, bimetallic Pt–Pd catalysts on acidic supports, such as Al_2O_3 [6], HY-zeolite [7–9,11,13,24,25], borosilicate [12], mordenite [10,22], SiO_2–Al_2O_3 [26,27], and B_2O_3–Al_2O_3 [28] have been reported as high-sulfur-tolerance aromatic hydrogenation catalysts. It was proposed that the high sulfur tolerance of noble metals supported on acidic supports should be attributed to the electron-deficient characteristic of noble metals resulting from the interaction with acidic (electron acceptor) support [29–32]. However, although the modified catalytic behavior of the Pt–Pd system exhibiting the high catalytic activity for aromatic hydrogenation has been reported by many researchers, it is still not clear why the Pt–Pd system has much higher activity than the monometallic Pt system and how it functions as compared to the monometallic one.

Extended X-ray absorption fine structure (EXAFS) spectroscopy is a powerful technique to characterize supported bimetallic catalysts, being especially useful for solving the evolution of the local structure around metal atoms [33]. Therefore, EXAFS seems to be a preferential tool for obtaining information about the active sites of bimetallic Pt–Pd catalysts.

In this paper, the catalytic activities of the bimetallic Pt–Pd/SiO_2–Al_2O_3 catalysts were examined for the aromatic hydrogenation of two different kinds of hydrotreated light cycle oil (LCO)/straight-run light gas oil (SRLGO) feedstock containing 29.4 vol% aromatics/31 ppm sulfur and 33.7 vol% aromatics/474 ppm sulfur under the industrial operating conditions. To examine the characteristics of the active sites of highly active Pt–Pd catalysts in detail, EXAFS measurements were carried out. The structure determination is performed by the experimental data of the EXAFS associated with the L_3-edge of Pt and K-edge of Pd.

Regarding both the activities of aromatic hydrogenation and the EXAFS results, it was concluded that the Pd species dispersed on Pt particles of the bimetallic Pt–Pd catalysts are the main active sites for the hydrogenation of aromatics in distillates.

2. Experimental

2.1. Preparation of catalysts

The support material used was SiO_2–Al_2O_3 (surface area 363 m^2/g, pore volume 0.71 ml/g). Monometallic and bimetallic Pt and Pd catalysts were prepared by pore volume impregnation of the support, using an aqueous solution of $H_2PtCl_6 \cdot 6H_2O$ and $PdCl_2$ as the impregnating salt, in the presence of dilute hydrochloric acid. After impregnation these catalysts were dried and calcined in air at 773 K for 4 h. Prior to the activity tests, fresh catalysts were reduced in an H_2 flow at 623 K for 2 h. All catalysts that were prepared are shown in table 1. Specific surface area was determined from nitrogen adsorption at 78 K by the BET method (Belsorp 28, Bel Japan).

* To whom correspondence should be addressed.

Table 1
Chemical and physical properties of prepared catalysts.

Active metal (wt%)		Surface area (m^2/g)
Pt0.5	–	306
Pt0.5	Pd0.27	287
Pt0.5	Pd0.5	308
Pt0.5	Pd1.0	305
	Pd0.27	303
	Pd0.5	304
	Pd1.0	310
Pt0.5	Pd2.0	319
Pt0.5	Pd1.5	301
Pt1.5		308
Pt1.0	Pd0.5	307
	Pd1.5	310

Table 2
Feed properties of untreated LCO/SRLGO and hydrotreated LCO/SRLGO.

	LCO/SRLGO	Hydrotreated LCO/SRLGO	
		A	B
Sulfur (wtppm)	1.0×10^4	31	474
Nitrogen (wtppm)	200	4	44
Density (15 °C) (g/cm^3)	0.8713	0.8431	0.8466
Composition (vol%)			
Paraffins	55.9	70.6	66.3
Olefins	4.2	0	0
Total aromatics (vol%)	40.0	29.4	33.7
mono-	20.5	25.3	29.7
di-	17.3	3.6	3.5
tri-	2.2	0.5	0.5
Distillation (°C)			
IBP	171.5	176.5	176.5
50%	298.0	289.0	291.0
FBP	387.0	374.0	379.0

2.2. Feedstock properties

Feedstock for this work was prepared by mixing LCO and SRLGO obtained from Cosmo Oil Sakai refinery. LCO is a middle distillate refinery product generated in a fluid catalytic cracking (FCC) unit. The mixing ratio of LCO/SRLGO in the feed oil was 30 vol%/70 vol%. Because of the high sulfur content (1.0 wt%) of LCO/SRLGO, noble-metal catalysts have to be used in the latter reactor of the two-stage hydrotreating process. Therefore, the LCO/SRLGO feed was previously hydrotreated using a CoMoP/HY zeolite–alumina catalyst (C-603A of Cosmo Oil [34,35]) before performing the hydrogenation experiments with the different noble-metal catalysts. The general properties of the untreated and hydrotreated LCO/SRLGO are given in table 2.

2.3. Equipment

Hydrogenation runs were carried out with an isothermal fixed-bed reactor (catalyst volume: 5 ml) operating in down-flow mode.

2.4. Reaction conditions

Hydrogenation of hydrotreated LCO/SRLGO feed was carried out under the following conditions: temperature 473 and 573 K, total pressure 4.9 MPa, liquid hourly space velocity (LHSV) 1.5 h^{-1}, and hydrogen-to-feed oil ratio 500 Nl/l.

2.5. Analytical

The percentages of aromatics content in feed and products were measured by high-performance liquid chromatography (HPLC). The HPLC analysis was performed using two types of detectors: ultraviolet (UV-8200, Tosoh Co.) and refractive index (RI-8200, Tosoh Co.) to measure quantitatively different types of aromatics, that is, mono, di, tri and total aromatics.

2.6. Kinetic calculations

The decrease in the total aromatics content in distillates was assumed to be pseudo-first-order. The following equation was used to analyze the results of each experiment:

$$k = \ln\left(\frac{C_\mathrm{f}}{C_\mathrm{p}}\right) \times \mathrm{LHSV},$$

where k is the hydrogenation rate (h^{-1}), C_p the amount of aromatics in the product, and C_f the amount of aromatics in the feedstock.

2.7. EXAFS measurement

The EXAFS spectra of Pt L_3-edge and Pd K-edge for Pt–Pd/SiO_2–Al_2O_3 catalysts were measured using the Si(311) double-crystal monochromator at a BL-10B station of the Photon Factory of the Institute of Materials Structure Science (KEK-PF) in Tsukuba, Japan. All measurements were performed at room temperature using the EXAFS cell (an optical path length of 7–15 mm, polyimide film windows), enabling *in situ* reducing and measurements. Catalyst samples were finely ground and mounted in an EXAFS cell. The samples were reduced in an H_2 stream (50 $cm^3\,min^{-1}$) under atmospheric pressure. During this reduction, the temperature was increased at a rate of 10 K/min to 623 K and then kept at 623 K for 2 h. After reducing, the samples were cooled to room temperature under flowing H_2. The samples were then evacuated at room temperature in order to remove all H_2 gas and sealed under vacuum (1×10^{-1} Pa).

Fourier transformation of the $k^3\chi(k)$ was performed in the k range of 8.2 $Å^{-1}$ for Pt L_3-edge and Pd K-edge [36]. Inverse Fourier transform was performed in the R range of 1.7–3.1 Å for Pt L_3-edge and 1.0–2.9 Å for Pd K-edge. Curve fitting for the Fourier-filtered $k^3\chi(k)$ was performed by using experimental spectra for Pt–Pt, Pt–Cl, Pd–Pd, Pd–O, and Pd–Cl pairs and theoretically calculated spectra for Pt–Pd and Pd–Pt pairs generated with the FEFF

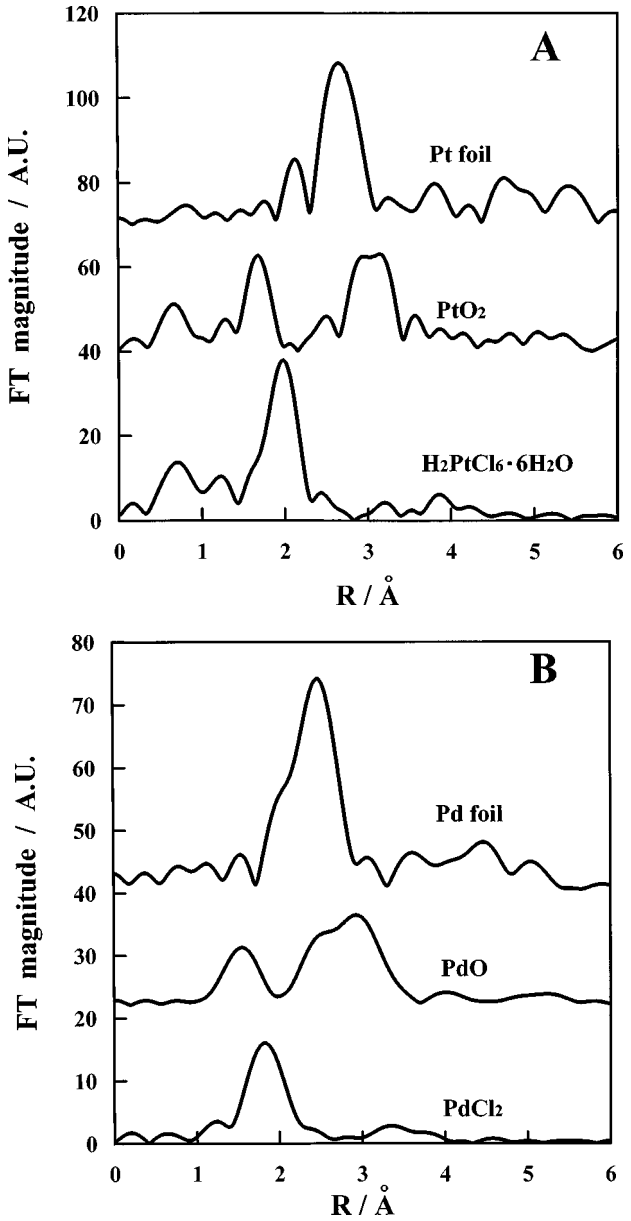

Figure 1. Fourier transforms of (A) Pt L_3-edge and (B) Pd K-edge EXAFS spectra for the model compounds (Pt foil, PtO_2, $H_2PtCl_6{\cdot}6H_2O$, Pd foil, PdO, and $PdCl_2$).

program [37–39]. Experimental spectra for Pt–Pt, Pt–O, Pt–Cl, Pd–Pd, Pd–O, and Pd–Cl pairs were obtained from Pt foil, PtO_2, $H_2PtCl_6{\cdot}6H_2O$, Pd foil, PdO, and $PdCl_2$. Figure 1 (A) and (B) shows Fourier transforms of Pt L_3-edge and Pd K-edge EXAFS spectra for the model compounds.

3. Results and discussion

3.1. Effect of Pd loading over Pt–Pd/SiO_2–Al_2O_3 catalyst

To investigate the effect of Pd loading on the hydrogenation activity, we examined the hydrogenation rate constants as a function of Pd loading of the Pt–Pd/SiO_2–Al_2O_3 catalyst. The Pt loading was held constant at 0.5 wt% as the Pd

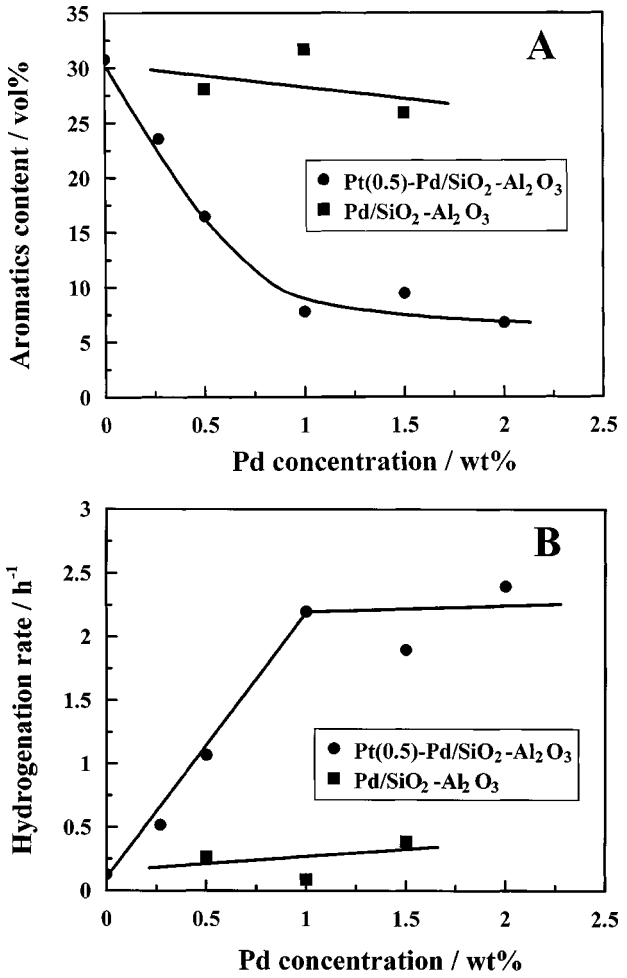

Figure 2. The effect of Pd loading over Pt–Pd/SiO_2–Al_2O_3 and Pd/SiO_2–Al_2O_3 catalysts. (A) Pd concentration versus aromatic content in product. (B) Pd concentration versus rate constant. Reaction conditions: feed hydrotreated LCO/SRLGO (474 ppm sulfur); temperature 573 K, hydrogen pressure 4.9 MPa; LHSV 1.5 h^{-1}; 8 days on stream.

concentration was varied. Also, Pd/SiO_2–Al_2O_3 catalysts without added Pt were prepared to compare with the Pt–Pd/SiO_2–Al_2O_3 catalysts. The activity measurements were carried out with hydrotreated LCO/SRLGO (474 ppm sulfur) at 573 K and a hydrogen pressure of 4.9 MPa. The amount of aromatics in product and the first-order rate constants for the catalysts are shown in figure 2 (A) and (B). Figure 2(A) indicates that aromatics content decreases significantly with Pd content in the case of the Pt–Pd/SiO_2–Al_2O_3 catalysts. As shown in figure 2(B), in the case of Pt–Pd/SiO_2–Al_2O_3, the hydrogenation activity increased linearly with the Pd content. On the other hand, in the case of Pd/SiO_2–Al_2O_3, which did not contain Pt, the substantial improvement in hydrogenation activity was not seen with an increase in Pd content. When the quantity of Pd is identical even if it adds the hydrogenation rate constant of Pd/SiO_2–Al_2O_3 to that of Pt(0.5 wt%)/SiO_2–Al_2O_3, it does not reach that of Pt–Pd/SiO_2–Al_2O_3. Therefore, it is assumed that there is an interaction of Pt and Pd in the Pt–Pd/SiO_2–Al_2O_3 catalysts and it improves the hydrogenation activity of aromatics in distillates.

The catalytic activity increased with the increase of Pd loading up to about 1.0 wt%, and then the activity became constant for a loading above 1.0 wt%. Thus, it can be concluded that 1.0 wt% loading of Pd on Pt(0.5 wt%)–Pd/SiO_2–Al_2O_3 is sufficient for obtaining the optimum catalytic performance. It is assumed that surplus Pd does not contribute to the hydrogenation activity. Therefore, it is concluded that the ratio of Pt and Pd must be precisely controlled to avoid the formation of wasteful Pd, as it does not contribute to the hydrogenation activity.

3.2. Dependence of the amount of sulfur in the feed

To investigate the dependence of the amount of sulfur in the feed, activity measurements were carried out over the catalysts with varied Pd/(Pt + Pd) atomic ratio with hydrotreated LCO/SRLGO (31, 474 ppm sulfur) at 473 and 573 K and a hydrogen pressure of 4.9 MPa. Because the hydrogenation activity with hydrotreated LCO/SRLGO (31 ppm sulfur) is much faster than that with hydrotreated LCO/SRLGO (474 ppm sulfur), the activity measurements with hydrotreated LCO/SRLGO (31 ppm sulfur) were performed at lower temperature. The first-order rate constants for the catalysts are shown in figure 3 (A) and (B). It can be seen that the hydrogenation activity for aromatics increased up to a maximum at about 4/5 of Pd/(Pt + Pd) atomic ratio and then decreased with a further increase in the Pd/(Pt + Pd) atomic ratio. Thus, the Pd/(Pt + Pd) atomic ratio that provided the highest catalytic properties was 4/5. In good agreement with this work, Yasuda et al. also found that the optimum point of the ratio of Pt and Pd over the USY-zeolite for the hydrogenation of tetralin containing dibenzothiophene is 4/5 [24]. Therefore, it is assumed that the active metal phase on SiO_2–Al_2O_3 is similar to that on USY-zeolite.

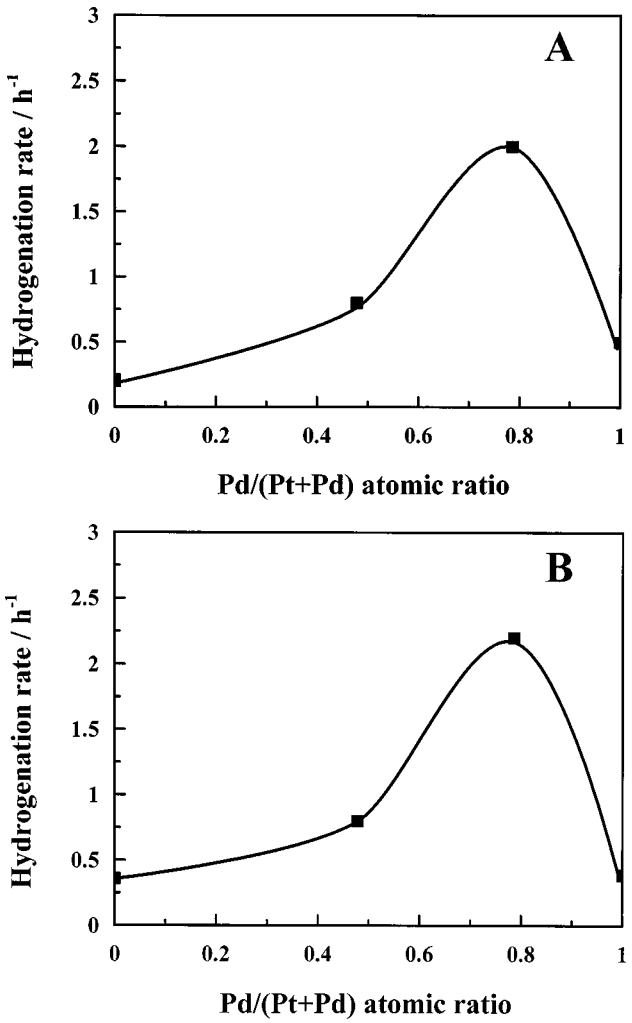

Figure 3. The effect of the Pd/(Pt + Pd) atomic ratio on the activity for the hydrogenation over Pt–Pd/SiO_2–Al_2O_3 catalysts. (A) Reaction conditions: feed hydrotreated LCO/SRLGO (31 ppm sulfur); temperature 473 K, hydrogen pressure 4.9 MPa; LHSV 1.5 h^{-1}; 8 days on stream. (B) Reaction conditions: feed hydrotreated LCO/SRLGO (474 ppm sulfur); temperature 573 K, hydrogen pressure 4.9 MPa; LHSV 1.5 h^{-1}; 8 days on stream.

The curve shape of the activity measurements carried out with hydrotreated LCO/SRLGO (31 ppm sulfur) is the same as that with hydrotreated LCO/SRLGO (474 ppm sulfur). It is demonstrated that the catalytic activities of bimetallic Pt–Pd and monometallic Pt and Pd catalysts were similarly affected by the concentration of the sulfur in feed. Therefore, it is clear that the bimetallic Pt–Pd system does not improve the sulfur tolerance as compared with the monometallic Pt or Pd system but it significantly enhances the intrinsic catalytic activity for aromatic hydrogenation.

3.3. EXAFS measurement

To investigate the local structures of the active metal phase, EXAFS measurements were carried out on Pd (1.5 wt%)/SiO_2–Al_2O_3 (Pd/(Pt + Pd) = 1), Pt(0.5 wt%)–Pd(1.0 wt%)/SiO_2–Al_2O_3 (Pd/(Pt + Pd) = ca. 4/5), Pt (1.0 wt%)–Pd(0.5 wt%)/SiO_2–Al_2O_3 (Pd/(Pt + Pd) = ca. 1/2), and Pt(1.5 wt%)/SiO_2–Al_2O_3 (Pd/(Pt + Pd) = 0) catalysts.

Figure 4 (A) and (B) shows the Fourier transforms of Pt L_3-edge and Pd K-edge EXAFS spectra for each catalyst reduced in an H_2 flow at 623 K. The Pt and Pd data in figure 4 (A) and (B) were inverse Fourier transformed. Furthermore, curve-fitting for the Fourier-filtered $k^3\chi(k)$ was performed by using experimental and theoretically calculated spectra. Table 3 indicates the structure parameters (coordination number and mean distance) calculated from the analysis of EXAFS oscillations. It is clear that there is a Pt–Pd bond on the Pt(0.5 wt%)–Pd(1.0 wt%)/SiO_2–Al_2O_3 and Pt(1.0 wt%)–Pd(0.5 wt%)/SiO_2–Al_2O_3 catalysts. Thus, it is concluded that the metal particles are not composed of mixtures of Pt and Pd particles, but each metal particle is composed of both Pt and Pd metals. Also, as compared with the coordination numbers of Pd–Pd and Pt–Pt bonds in Pt(0.5 wt%)–Pd(1.0 wt%)/SiO_2–Al_2O_3 and Pt(1.0 wt%)–Pd(0.5 wt%)/SiO_2–Al_2O_3 catalysts, the coordination number of the Pt–Pt bond exceeds that of the Pd–Pd bond. Hansen et al. [40] confirmed that the coordination number

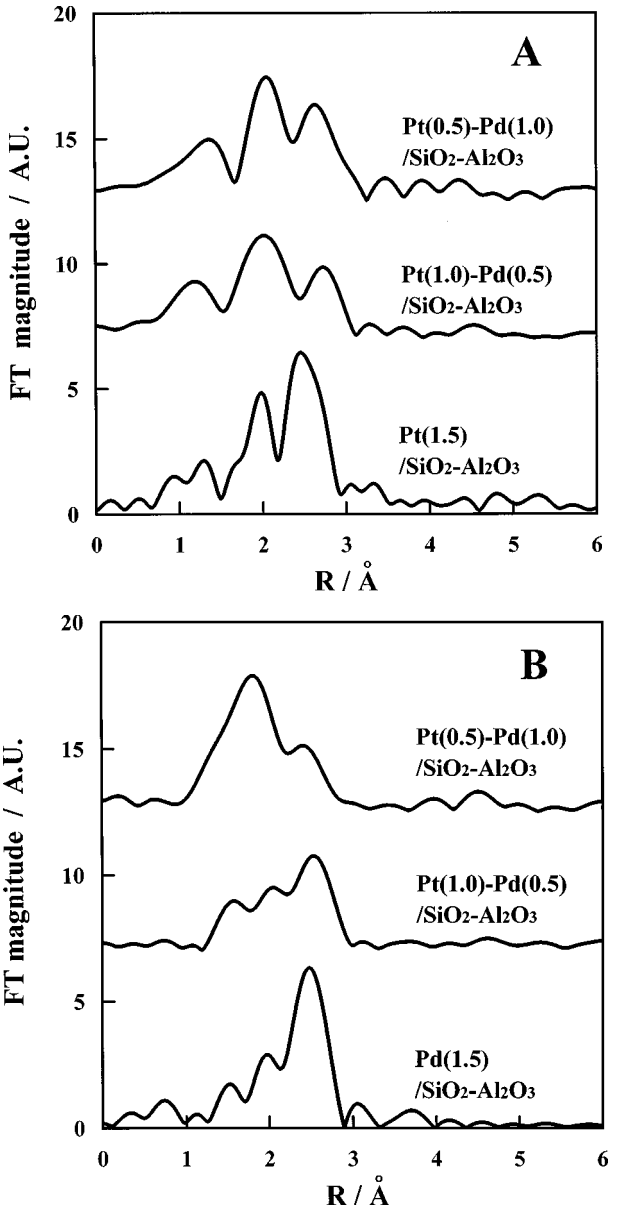

Figure 4. Fourier transforms of (A) Pt L_3-edge and (B) Pd K-edge EXAFS spectra for Pd(1.5 wt%)/SiO_2–Al_2O_3, Pt(0.5 wt%)–Pd(1.0 wt%)/SiO_2–Al_2O_3, Pt(1.0 wt%)–Pd(0.5 wt%), and Pt(1.5 wt%)/SiO_2–Al_2O_3 catalysts reduced in an H_2 flow at 623 K.

of the Pt–Pt bond exceeds that of the Pd–Pd bond when Pd exists on the surface of a Pt–Pd bimetallic particle. Toshima et al. [41–44] reported that the results of X-ray diffraction, X-ray photoelectron spectroscopy, and EXAFS on the Pd/Pt (4/1 and 1/1 mol ratios) bimetallic clusters in the colloidal dispersions indicated the "Pd-surrounded Pt core structure", in which the 42 Pd atoms are on the surface of the cluster particle and 13 Pt atoms are at the center of the particle, forming a core. The structure parameters of the colloidal dispersions of the Pd/(Pt + Pd) (4/5 and 1/2 atomic ratios) bimetallic clusters determined by Toshima et al. [41] are in good agreement with those of Pt(0.5 wt%)–Pd(1.0 wt%)/SiO_2–Al_2O_3, of which the Pd/(Pt+Pd) atomic ratio is ca. 4/5, and Pt(1.0 wt%)–Pd(0.5 wt%)/SiO_2–Al_2O_3,

Table 3
Structure parameters of Pt–Pd/SiO_2–Al_2O_3 catalysts.

Catalyst	Bond	R (Å)	Coordination number
Pd(1.5)	Pd–Pd	2.75	4.6
Pt(0.5)–Pd(1.0)	Pt–Pd	2.71	4.2
	Pt–Pt	2.73	4.2
	Pd–Pt	2.71	1.1
	Pd–O	2.03	1.3
	Pd–Cl	2.32	1.2
	Pd–Pd	2.71	1.6
Pt(1.0)–Pd(0.5)	Pt–Pd	2.68	2.6
	Pt–Pt	2.69	5.7
	Pd–Pt	2.68	2.6
	Pd–O	2.10	0.8
	Pd–Cl	2.43	0.4
	Pd–Pd	2.77	1.4
Pt(1.5)	Pt–Cl	2.32	2.3
	Pt–Pt	2.69	5.3

of which the Pd/(Pt + Pd) atomic ratio is ca. 1/2, in our work. Therefore, it may be presumed that the active metal particles on the Pt–Pd/SiO_2–Al_2O_3 catalysts are composed of the Pd species dispersed on Pt particles. In light of this assumption, it is reasonable to consider that in the case of Pt–Pd/SiO_2–Al_2O_3, the hydrogenation activity increased linearly with the increase in the Pd loading, as shown in figure 2(B). It is highly probable that the main active site for aromatic hydrogenation is the surface Pd on the Pt–Pd metal particles. Therefore, surplus Pd, which does not interact with a Pt particle, is not responsible for the high activity for aromatic hydrogenation.

Also, in the case of Pt–Pd/SiO_2–Al_2O_3 catalysts, the Pd–Cl bond and Pd–O bond were observed. It is assumed that the Pd metals easily combined with the Cl and O atoms on the support, because the Pd atoms exist on the surface of the metal particles. However, in the case of the Pd(1.5 wt%)/SiO_2–Al_2O_3 catalysts, Pd–Cl and Pd–O bonds were not observed. Although it is necessary to perform further detailed investigations, we imagine that in the case of the monometallic Pd catalyst, Pd–Cl and Pd–O bonds were not formed, because the Pd metal particles were readily reduced, while, in the case of bimetallic Pt–Pd catalysts, Pd–Cl, and Pd–O bonds were formed, since the ligand effect of Pt upon the Pd of the surface took place and the surface Pd on the metal particles became poorer in electronic density than in the Pt core.

There is a general agreement in the literature [45–47] that the dispersion of Pt is higher than that of Pd. However, table 3 shows that the coordination number (5.3) for supported monometallic Pt is higher than that (4.6) for supported monometallic Pd. In general, this means that the Pd catalyst has a higher dispersion than the Pt one.

In this study, we also performed TEM measurements of Pt(1.5 wt%)/SiO_2–Al_2O_3, Pt(0.5 wt%)–Pd(1.0 wt%)/SiO_2–Al_2O_3, Pt(1.0 wt%)–Pd(0.5 wt%)/SiO_2–Al_2O_3, and Pd(1.5 wt%)/SiO_2–Al_2O_3 after reduction under the same

conditions. From the results, the particle size of clusters of each catalyst was, respectively, about 10 Å for Pt(1.5 wt%)/SiO_2–Al_2O_3, 10 Å or less for Pt (0.5 wt%)–Pd(1.0 wt%)/SiO_2–Al_2O_3, 10–20 Å for Pt(1.0 wt%)–Pd(0.5 wt%)/SiO_2–Al_2O_3, and 70–200 Å for Pd(1.5 wt%)/SiO_2–Al_2O_3. The results of the TEM measurements are in disagreement with those of the EXAFS measurements. Therefore, we think that the primary particles of Pd in the absence of Pt easily gather and form agglomerations (secondary particles) without a change of coordination number. The EXAFS and the TEM studies lead to the suggestion that Pt in the Pt–Pd bimetallic system retards the formation of Pd agglomerations and further is regarded as a support for dispersing the active Pd species.

The current literature does not agree with our opinion: Chang et al. [48] proposed that the effect of Pd in Pt–Pd/Al_2O_3 is to decrease the electron density of Pt and thereby improve the sulfur tolerance of supported Pt catalysts. However, if the main active site is Pt and the role of Pd is only to modify the electronic properties of Pt, it is difficult to explain why the hydrogenation activity of the bimetallic Pt–Pd system increased linearly with the increase in the Pd loading in figure 2(B). Therefore, we propose that the main active sites for aromatic hydrogenation are the Pd species dispersed on Pt particles in the bimetallic Pt–Pd system.

4. Conclusions

In order to examine the characteristics of the active sites of highly active Pt–Pd catalysts in detail, we performed activity measurements of the Pt–Pd/SiO_2–Al_2O_3 catalysts with hydrotreated LCO/SRLGO feedstock (31, 474 ppm sulfur) under industrial hydrogenation conditions and studies of the active sites with EXAFS. The main conclusions of this work are summarized as follows:

(1) Bimetallic Pt–Pd/SiO_2–Al_2O_3 catalysts exhibited much higher activities in aromatic hydrogenation of distillates than monometallic Pt and Pd/SiO_2–Al_2O_3 catalysts.

(2) Bimetallic Pt–Pd system does not improve the sulfur tolerance as compared with monometallic Pt or Pd system but it significantly enhances the intrinsic catalytic activity for aromatic hydrogenation.

(3) The EXAFS studies indicated that there is an interaction between Pt and Pd in the Pt–Pd/SiO_2–Al_2O_3 catalyst.

(4) From the EXAFS, it was assumed that the active metal particles on the Pt–Pd/SiO_2–Al_2O_3 catalysts are composed of the Pd species dispersed on Pt particles.

(5) Regarding the activities of aromatic hydrogenation, it was assumed that the Pd sites dispersed on Pt particles were responsible for the high activity of the bimetallic Pt–Pd/SiO_2–Al_2O_3 catalysts.

Acknowledgement

This R&D was supported by the Petroleum Energy Center (PEC), under the sponsorship of the Ministry of International Trade and Industry (MITI) of Japan. This EXAFS experiment was done under the permission of the Photon Factory of the Institute of Materials Structure Science (Proposal No. 97Y007). The authors thank Professors Toshiaki Ohta and Toshihiko Yokoyama of the University of Tokyo for their helpful discussions and for the use of their data analysis program on the EXAFS measurements.

References

[1] T.L. Ullman, SAE Paper No. 892072 (1989).
[2] R. Lindsay, J.M. Marriott, M. Booth and C.V. Paassen, Petrol. Rev. (July 1992) 320.
[3] A. Stanislaus and B.H. Cooper, Catal. Rev. Sci. Eng. 36 (1994) 75.
[4] B.H. Cooper and B.B.L. Donnis, Appl. Catal. A 137 (1996) 203.
[5] B.H. Cooper, A. Stanislaus and P.N. Hannerrup, Am. Chem. Soc. Div. Fuel Chem. Preprints 37 (1992) 41.
[6] S.M. Kovach and G.D. Wilson, US Patent 3 943 053 (1976), to Ashland Oil, Inc.
[7] D. Hamilton, US Patent 4 640 764 (1987), to Shell Oil Company.
[8] P.J. Angevine and S.M. Clark, US Patent 4 683 214 (1987), to Mobil Oil Corp.
[9] J.K. Minderhoud and J.P. Lucien, Eur. Patent 303 332 (1988), to Shell IRM.
[10] S.G. Kukes, F.T. Clark, P.D. Hopkins and L.M. Green, US Patent 5 151 172 (1991), to Amoco Corp.
[11] S.G. Kukes, F.T. Clark and P.D. Hopkins, US Patent 5 147 526 (1992), to Amoco Corp.
[12] F.T. Clark, S.G. Kukes and P.D. Hopkins, US Patent 5 271 828 (1993), to Amoco Corp.
[13] S.G. Kukes, F.T. Clark and P.D. Hopkins, US Patent 5 308 814 (1994), to Amoco Corp.
[14] J. Heinerman and E. Vogt, PCT Int. Patent Appl. WO 94/26846 (1994).
[15] T. Enomoto, Y. Nakatsuka, T. Ino and M. Hatayama, Eur. Patent Appl. 0724474A2 (1996).
[16] A.J. Suchanek and G.L. Hamilton, AM-91-35, NPRA Annual Meeting, March 1991.
[17] P.S. Andersen, B.H. Cooper and P.N. Hannerup, AM-92-50, NPRA Annual Meeting, March 1992.
[18] J.P. Lucien, J.P. van der Berg, G. Germine, H.M.J.H. van Hooijdonk, M. Gjers and G.L.B. Thielmans, in: *Catalytic Hydroprocessing of Petroleum and Distillations*, eds. M.C. Oballa and S.S. Shih (Dekker, New York, 1994) p. 291.
[19] W.H.J. Stork, Am. Chem. Soc. Symp. Ser. 634 (1996) 379.
[20] B.H. Cooper, P.N. Hannerup and P.S. Andersen, Erdol Kohle. Erdgas. Petrochem. 47 (1994) 330.
[21] A. Corma, A. Martinez and V. Martinez-Sria, J. Catal. 169 (1997) 480.
[22] C. Song and A.D. Schmitz, Energy Fuels 11 (1997) 656.
[23] R. Navarro, B. Pawelec, J.L.G. Fierro, P.T. Vasudevan, J.F. Cambra and P.L. Arias, Appl. Catal. A 137 (1996) 269.
[24] H. Yasuda and Y. Yoshimura, Catal. Lett. 46 (1997) 43.
[25] H. Yasuda, N. Matsubayashi, T. Sato and Y. Yoshimura, Catal. Lett. 54 (1998) 23.
[26] T. Fujikawa, K. Idei, T. Ebihara, H. Mizuguchi and K. Usui, Appl. Catal. A, to be accepted.
[27] M. Vaarkamp, B.H. Reesink and P.H. Berben, PCT Int. Patent Appl. WO 98/35754 (1998).
[28] T. Fujikawa, K. Idei and K. Usui, J. Jpn. Petrol. Inst. 42 (1999) 271.

[29] R.A. Dalla Betta and M. Boudart, in: *Proc. 5th Int. Congr. Catal.*, Vol. 2 (North-Holland, Amsterdam, 1972) p. 1329.
[30] R.A. Dalla Betta, M. Boudart, P. Gallezot and R.S. Weber, J. Catal. 69 (1981) 524.
[31] P. Gallezot and G. Bergeret, in: *Catalyst Deactivation*, eds. E.E. Peterson and A.T. Bell (Dekker, New York, 1987) p. 263.
[32] S.T. Homeyer, Z. Karpinski and W.M.H. Sachtler, J. Catal. 123 (1990) 60.
[33] J.H. Sinfelt, in: *Bimetallic Catalysts: Discoveries, Concepts, and Applications* (Wiley, New York, 1983).
[34] T. Fujikawa, O. Chiyoda, M. Tsukagoshi, K. Idei and S. Takehara, Catal. Today 45 (1998) 307.
[35] T. Fujikawa, O. Chiyoda, K. Idei, T. Yoshizawa and K. Usui, Stud. Surf. Sci. Catal. 121 (1999) 277.
[36] T. Yokoyama, H. Hamamatsu and T. Ohta, Program "EXAFSH", version 2.2, The University of Tokyo.
[37] J.J. Rehr, R.C. Albers and J. Mustre de Leon, Physica B 158 (1989) 417.
[38] J.J. Rehr, J. Mustre de Leon, S.I. Zabinsky and R.C. Albers, J. Am. Chem. Soc. 113 (1991) 5135.
[39] A. Ankudinov, Ph.D. dissertation, University of Washington (1996).
[40] P.L. Hansen, A.M. MolenBloek and A.V. Ruban, J. Phys. Chem. B 101 (1997) 1861.
[41] N. Toshima, M. Harada, T. Yonezawa, K. Kushibiki and K. Asakura, J. Phys. Chem. 95 (1991) 7448.
[42] M. Harada, K. Asakura, Y. Ueki and N. Toshima, J. Phys. Chem. 96 (1992) 9730.
[43] N. Toshima, M. Harada, Y. Yamazaki and K. Asakura, J. Phys. Chem. 96 (1992) 9927.
[44] N. Toshima, T. Yonezawa and K. Kushibiki, J. Chem. Soc. Faraday Trans. 89 (1993) 2537.
[45] D. Poondi and M.A. Vannice, J. Catal. 161 (1996) 742.
[46] E. Blomsma, J.A. Martens and P.A. Jacobs, J. Catal. 165 (1997) 241.
[47] J.K. Lee and H.K. Rhee, J. Catal. 177 (1998) 208.
[48] T.B. Lin, C.A. Jan and J.R. Chang, Ind. Eng. Chem. Res. 34 (1995) 4284.